Description of 3α-bosonic states in the ^{12}C nucleus with local and nonlocal potentials

R. Lazauskas and M. Dufour
IPHC Bat27, IN2P3-CNRS/Université Louis Pasteur BP28, F-67037 Strasbourg Cedex 2, France
(Received 7 October 2011; revised manuscript received 2 December 2011; published 19 December 2011)

The ^{12}C nucleus is investigated in a nonmicroscopic α-particle model involving local and nonlocal potentials. Faddeev equations formulated in configuration space are used to solve the three-body problem for bound and resonant states. We demonstrate that the nonlocal potential developed by Papp and Moszkowski [Mod. Phys. Lett. B **22**, 2201 (2008)] appears to be particularly well adapted to study 3α clustering. We point out ^{12}C states of positive-parity which share common features with the 0_2^+ Hoyle states. Several negative-parity states revealing a clear bosonic α-particle structure are also obtained.

DOI: 10.1103/PhysRevC.84.064318 PACS number(s): 21.60.Gx, 21.45.−v, 03.75.Hh, 21.10.Dr

I. INTRODUCTION

The description of the atomic nucleus as a quantum system of interacting nucleons is a fundamental problem of theoretical nuclear physics. Nucleons being fermions, the corresponding A-body wave functions must be correctly antisymmetrized to take the Pauli principle into account. In such so-called microscopic models, the structure in quarks of the nucleons is neglected. Shell models, or microscopic cluster models, are typical examples of such approaches [1].

However, the α particle has played a special role since the early days of nuclear physics [2,3]. Experimentally, α-particle clustering effects are currently well established in light nuclei. Owing to its compactness and strong binding, the idea that the α particle tends to keep its own identity inside the nucleus is at the origin of cluster models. According to the description of the α particle as a composite particle or as an elementary one, microscopic and nonmicroscopic theoretical frameworks have been developed.

In the microscopic approach, the α particle is usually seen as two neutrons and two protons that fill up the s shell of a harmonic oscillator potential (one cluster). Historically, the description of nuclear states based on such a cluster structure was first suggested by Wheeler [4] and by Margenau [5], then extended by Brink [6]. The first applications were devoted to the study of α-particle nuclei (i.e., ${}^{4n}_{2n}X$-type nuclei, with nucleon number $A = 4n$, such as ^{8}Be, ^{12}C, or ^{16}O nuclei). In such cases, the Pauli principle is exactly treated through antisymmetrization of the A-nucleon wave functions.

In addition, the total angular momentum of the α particle is zero and therefore it must be treated as a boson in nonmicroscopic models [2]. Because of its bosonic nature, the wave functions of the whole system must be symmetric for exchange of any two α particles.

The transition from descriptions in terms of A fermions toward those in terms of n bosons is far from obvious. However, it remains a very interesting challenge, which can help to point out states in which α clustering is expected to be strongly dominant, such as in the so-called condensate state [7], a typical example being the 0_2^+ in the ^{12}C nucleus, known as the Hoyle state [8], which plays a crucial role in stellar nucleosynthesis processes.

Numerous works have been devoted to this subject, particularly to the study of the ^{12}C nucleus viewed either as a system of 12 nucleons or as a system of 3 α particles. It is impossible to give here an exhaustive list of all of them. We just mention some of the representative ones. For the microscopic aspects, we cite studies performed using the resonating group method (RGM) [9], with the generator coordinate method [10], and employing antisymmetrized molecular dynamics [11] and fermionic molecular dynamics [12]. For nonmicroscopic approaches, different methods have been used, such as the orthogonality condition method (OCM) [13]. This method presents a simplified version of the RGM where the antisymmetrization is approximatively taken into account through the orthogonality with the forbidden states. Two typical applications using the OCM are the study by Yamada and Schuck [14], which focuses on the condensate interpretation of four states around the 3α threshold, and the study by Kurukawa and Katō [15,16], which investigates 3α-cluster structure in the ^{12}C nucleus. Let us also mention the two recent works of Alvarez-Rodriguez *et al.* [17] and Descouvemont using the formalism of hyperspherical harmonics [18].

In spite of all these investigations, the physical problem is still far from being well mastered. For the nonmicroscopic approaches the most important challenge is to replace forces acting between nucleons by phenomenological potentials between the α particles. These forces must be able to simulate not only the internal structure of the α particle but also, and most importantly, the Pauli principle between the single nucleons. In such a context, several local and nonlocal potentials have been developed.

A straightforward approach is to parametrize a local shallow α-α potential consistent with the nonexistence of the ^{8}Be bound state, which reproduces experimental $\alpha\alpha$ phase shifts together with energies of near-threshold ^{8}Be resonances. One way to simulate the Pauli principle is to define potentials with a strong repulsive core, which was done by Ali and Bodmer in the 1960s [19]. Nevertheless, such an approach seems to be far from being satisfactory because it leads to a strong underbinding of the ^{12}C ground state (see Refs. [18,20] and references therein).

An alternative approach is to consider a local deep potential, such as the potential proposed by Buck *et al.* [21]. It is

well known that such interactions involve nonphysical Pauli-forbidden 2α bound states which must be eliminated by an appropriate projection procedure [20,22]. Until now, however, there has been no unique prescription of how to project out these states. One way is to use a projector constructed using two-body eigenfunctions of these states. Another way is to use Pauli-forbidden relative motion states consistent with a shell-model description of 2α particles [22]. The first prescription leads to a strong underbinding of the ^{12}C ground-state nucleus, similar to that obtained by the shallow Ali-Bodmer potential [18,23]. On the contrary, the second prescription leads to a significant overbinding of the ^{12}C ground state [18,24,25].

To improve previous descriptions, one is obliged to recourse to three-body forces. However, works already performed in that direction reveal the necessity of three-body forces with either rather complex structure and/or being dependent on the angular momentum J [16,18]. In such conditions, the definition of phenomenological multibody forces seems unavoidable in describing heavier multi-α-particle structures [26]. This point is of course a serious drawback for nonmicroscopic approaches.

The most elaborate prescription to account for nucleon structure in the nonmicroscopic description of nuclear clusters is provided by the so-called fish-bone optical model [27–29]. This model takes into consideration not only fully Pauli forbidden states of relative motion between the clusters but also partially Pauli forbidden states and thus may be considered an extension of the OCM. It was demonstrated that the fish-bone model agrees with the resonating group model up to the omission of some residual interaction [28]. In such a context, a very accurate parametrization of the α-α fish-bone potential was realized recently by Papp and Moszkowski [30]. Using a single parameter set for each partial wave, these authors succeeded in reproducing together the $\ell = 0$, $\ell = 2$, and $\ell = 4\alpha$-α phase shifts up to 20 MeV, the $E_{2\alpha} = 91.6$ keV resonance in the ^{8}Be nucleus, as well as the ground-state binding energy of the ^{12}C. A notable feat of this work is the ability to describe the two lowest 0^+ ^{12}C states without resorting to three-body force.

The present paper aims to investigate bound and resonant states of both positive and negative parity of the ^{12}C nucleus in a nonmicroscopic 3α-particle model. The nonrelativistic quantum three-body problem is solved using the formalism of the Faddeev equations [31] in configuration space. The nonlocal Papp and Moszkowski potential [30] is chosen to model the two-body interactions between the α particles. We generalize the calculation of Ref. [30] where 3α calculations are limited to the two lowest 0^+ states of the ^{12}C nucleus. A determination of resonant-state energies and widths is performed by employing the complex-scaling method [32,33]. Furthermore, we complement our investigations with calculations involving the Ali and Bodmer potential [19] completed by new three-body forces.

Our calculations focus particularly on $(J, T = 0)$ resonances located above the 3α threshold, which are expected to present a bosonic α structure. Among them, the most famous one is the aforementioned 0^+_2 Hoyle state located at $E_{3\alpha} = 0.38$ MeV. This state was known for a long time to manifest a well-developed 3α-cluster structure. It cannot be reproduced currently by standard approaches such as the shell model even in its no-core version [34], but it was successfully described by several microscopic-cluster models (see Refs. [10,11] and references therein). Let us also mention a recent investigation with an *ab initio* calculation within an effective field-theory theoretical framework [35].

The interest in the Hoyle state in particular was revived recently with its interpretation as an α-condensate state in analogy with the Bose-Einstein condensate [7]. A related question is to know if it can be considered a rotational bandhead. In such a context, the location of the 2^+ member was investigated by several experimental and theoretical approaches (see Refs. [16,36] and references therein). Experimentally, the most recent measure was performed by Freer *et al.* [36]. The predicted value of energy is $E_x = 9.6(1)$, with a width of $\Gamma = 0.6(1)$ MeV. This result is supported by several microscopic and nonmicroscopic theoretical calculations, which predict the 2^+ member at about 2–3 MeV above the 3α threshold (see Refs. [10,16] and references therein). In addition, let us also mention the existence of a very broad 0^+_3 state measured at $E_x \approx 10$ MeV with a width of $\approx$3 MeV [36,37]. This state was interpreted as a molecular 3α state and also as a possible condensate (suggested in Ref. [38]).

Negative-parity resonances are also interesting to investigate, both to address the quality of potentials mostly fitted on positive-parity states and to discuss the physical properties of resonances such as the 3^-_1, 2^-_1, and 1^-_1 states, which are also believed to present α clustering [14,16,38].

The present paper is organized as follows. Section II is devoted to the theoretical framework. Results with the nonlocal Papp and Moszkowski potential and with the Ali and Bodmer potential are discussed in Secs. III and IV, respectively. Concluding remarks are given in Sec. V.

II. THEORETICAL FRAMEWORK

The nonrelativistic quantum three-body problem is described by means of the Faddeev equations in configuration space [31]. With the hypothesis of three identical particles subject to pairwise interaction v_{ij} and three-body force W_{123}, written as a symmetric sum (with respect to the particle permutation) of three terms $W_{123} = w_{12,3} + w_{23,1} + w_{31,2}$, the Faddeev equations read

$$(E - \widehat{H}_0 - v_{ij})\psi_{ij,k} = v_{ij}(P^+ + P^-)\psi_{ij,k} + w_{ij,k}\Psi, \qquad (1)$$

where $\widehat{H}_0$ is the three-particle kinetic energy operator, $\psi_{ij,k}$ the Faddeev component, and P^+, P^- the cyclic particle permutation operators. The properly symmetrized three-body wave function is $\Psi = (1 + P^+ + P^-)\psi_{ij,k}$. It is easy to verify that the sum of the three Faddeev equations defined in Eq. (1) leads to the Schrödinger equation.

In this work, v_{ij} represents either the nonlocal Papp and Moszkowski potential [30] or the local Ali and Bodmer potential [19] complemented by the Coulomb force between the α particles. We do not recopy here the analytical expressions of these two potentials, which can be entirely found in Refs. [19,30].

Let us now summarize the main steps to solve Eq. (1), including the implementation of the complex scaling method. To simplify the kinetic energy operator and to separate internal and center-of-mass degrees of freedom we use the Jacobi coordinates defined as $\vec{x_{ij}} = \vec{r_j} - \vec{r_i}$ and $\vec{y_{ij}} = \frac{2}{\sqrt{3}}[\vec{r_k} - \frac{1}{2}(\vec{r_i} + \vec{r_j})]$.

The energy of the resonance states and the corresponding eigenfunctions are obtained by solving the following Schrödinger (or Faddeev) equation:

$$\widehat{H}\Psi_{\rm res} = E_{\rm res}\Psi_{\rm res}, \quad \text{with} \quad E_{\rm res} = \varepsilon_{\rm res} - \frac{i}{2}\Gamma_{\rm res}, \tag{2}$$

where $\widehat{H} = \widehat{H}_0 + v_{12} + v_{23} + v_{31} + W_{123}$ is the full three-body Hamiltonian.

Because physical resonances have positive-energy real parts ($\varepsilon_{\rm res} > 0$), the corresponding eigenfunctions are not square integrable. Nevertheless, by applying a similarity transformation, they can be mapped onto normalizable states. That is,

$$(\widehat{S}\widehat{H}\widehat{S}^{-1})(\widehat{S}\Psi_{\rm res}) = E_{\rm res}(\widehat{S}\Psi_{\rm res}) \tag{3}$$

with $\widehat{S}\Psi_{\rm res} \to 0$ as $r \to \infty$. Functions $(\widehat{S}\Psi_{\rm res})$ are then in Hilbert space, although $\Psi_{\rm res}$ are not. In the complex-scaling method [32,33], the similarity operator reads

$$\widehat{S} = e^{i\theta r\frac{\partial}{\partial r}} \tag{4}$$

such that any analytical function $f(r)$ is transformed according to

$$\widetilde{f}(r) = \widehat{S}f(r) = f(re^{i\theta}). \tag{5}$$

For a broad class of potentials, the complex-scaling operation does not affect the bound- and resonant-state spectra of the Hamiltonian $\widehat{H}$, provided $0 \leqslant \theta < \frac{\pi}{2}$. In addition, the continuous spectra of $\widehat{H}$ is rotated by an angle 2θ. Resonance eigenfunctions $(\widehat{S}\Psi_{\rm res})$ of the scaled Hamiltonian become square integrable if $\tan(2\theta) > \Gamma/2\epsilon_{\rm res}$ and therefore standard bound-state techniques can be applied to determine the corresponding eigenvalues.

Complex scaling of the Faddeev equations causes no difficulties. All the Jacobi vectors have simply to be scaled with the same exponential factor

$$\vec{x_{ij}} \to \vec{x_{ij}}e^{i\theta} \qquad \text{and} \qquad \vec{y_{ij}} \to \vec{y_{ij}}e^{i\theta}. \tag{6}$$

Such a transformation affects only the hyper-radius $\rho = \sqrt{x_{ij}^2 + y_{ij}^2}$ but not the angular dependence of the Faddeev equations or the expressions of the permutation operators (P^+, P^-). For instance, the complex-scaled kinetic-energy operator can be expressed as a six-dimensional Laplacian $\widehat{H}_0 = -(e^{-i2\theta})\frac{\hbar^2}{m}\Delta_\chi$ with $\chi \equiv (\vec{x_{ij}}, \vec{y_{ij}})$.

As in our previous works [39,40], we project the Faddeev components onto a partial-wave basis of the total angular momentum LM:

$$\widetilde{\psi}_{ij,k}(\vec{x_{ij}}, \vec{y_{ij}}) = \sum_{\ell_x,\ell_y} \frac{\psi^{LM}_{\ell_x\ell_y}(x_{ij}, y_{ij})}{x_{ij}y_{ij}} \left[Y_{\ell_x}(\widehat{x_{ij}}) \otimes Y_{\ell_y}(\widehat{y_{ij}})\right]_{LM}, \tag{7}$$

where ℓ_x and ℓ_y are the partial angular momenta associated with Jacobi coordinates $\vec{x}$ and $\vec{y}$, respectively.

Because the α particle has spin zero, no explicit spin dependence is required in the last expression. Moreover, the total angular momentum J of the 3α system coincides with the total orbital angular momentum L. Owing to the bosonic nature of the α particle, symmetrization implies that ℓ_x must be an even integer. No such restriction exists on ℓ_y values. It is also easy to verify that the parity of the 3α system obeys the following simple rule: $\pi = (-1)^{\ell_x+\ell_y} = (-1)^{\ell_y}$.

After the complex-scaling operation followed by the projection of Eq. (1) onto the partial-wave basis given in Eq. (7), one obtains a system of integro-differential equations. Next, the radial dependence of the amplitudes $\psi^{LM}_{\ell_x\ell_y}(x_{ij}, y_{ij})$ is developed onto a basis of cubic Hermite splines [41]. Such a procedure leads to a generalized algebraic eigenvalue problem written as

$$AX = E_{\rm res}BX, \tag{8}$$

where A and B are known complex matrices, and $E_{\rm res}$ and X are respectively the complex eigenvalue and eigenvector to be determined. In practice, A and B are large-scale matrices with typical dimension of $\approx 2 \times 10^4$. An inverse iteration method is used to determine the eigenvalues. This iterative method permits to determine the closest eigenvalue to the initial guess value. For more technical details about the numerical algorithm employed, interested readers may refer to Refs. [39,40]. We generally limited our investigations to about 10 MeV above the 3α threshold, which corresponds to the natural limit for the considered α-α interactions. (These interactions are generally derived by fitting α-α scattering data up to $E_{\rm c.m.} \sim 10$ MeV.)

In our calculations, the sum (7) is limited to $\ell_x^{\max} = \ell_y^{\max} = 8$. This choice guarantees at least three-digit accuracy. Initial values were carefully tested to eliminate the risk of losing a resonance and at least two scaling angles ($\theta = 6^\circ$ and $\theta = 10^\circ$) were systematically used to test the scaling.

Because resonance wave functions $\psi_{ij,k}$ are not square integrable, the calculation of the norm or of the mean value of some operators $\widehat{O}(\vec{x_{ij}}, \vec{y_{ij}})$ does not generally converge to a finite value. In addition, the complex-scaled functions $\widetilde{\psi}_{ij,k}$ turn out to be square integrable. We then use them to study the physical properties of the resonance wave-function internal part. To do that, we introduce complex-mean-value integrals involving the scaled functions and the scaled operators. In such a context, we define the complex norm as follows:

$$N = \iint \widetilde{\Psi}(\vec{x_{ij}}, \vec{y_{ij}})\widetilde{\Psi}(\vec{x_{ij}}, \vec{y_{ij}})d^3x_{ij}d^3y_{ij} \tag{9}$$

$$= 3\iint \widetilde{\psi}_{ij,k}(\vec{x_{ij}}, \vec{y_{ij}})\widetilde{\Psi}(\vec{x_{ij}}, \vec{y_{ij}})d^3x_{ij}d^3y_{ij}, \tag{10}$$

where the second equality results from the permutation symmetry of the three identical particles. Then the complex mean value of the operator $\widehat{O}(\vec{x_{ij}}, \vec{y_{ij}})$ is given by

$$\langle\widehat{O}\rangle = \frac{1}{N}\iint \widetilde{\Psi}(\vec{x_{ij}}, \vec{y_{ij}})\widehat{O}(\vec{x_{ij}}e^{i\theta}, \vec{y_{ij}}e^{i\theta}) \times \widetilde{\Psi}(\vec{x_{ij}}, \vec{y_{ij}})d^3x_{ij}d^3y_{ij}. \tag{11}$$

TABLE I. ^{12}C energies (in MeV), total widths (in MeV), and root-mean-square radius (in fermis) calculated with the Papp and Moszkowski potential (PM). 2_2^+ experimental data are taken from Ref. [36]. Other experimental data are taken from Ref. [43], where the (4^-) at $E_x = 13.352$ MeV is tentatively assigned to a 2^- state (see text).

J^π	E_x^{expt}	$E_{3\alpha}^{\text{expt}}$	Γ^{expt}	$E_{3\alpha}^{\text{PM}}$	Γ^{PM}	$\sqrt{r^2}^{\text{PM}}$
0_1^+	0	−7.2747		−7.27		2.40
2_1^+	4.43891(31)	−2.8358		−5.93		2.34
4_1^+	14.083(15)	6.8083	0.258(15)	−2.88		2.25
0_2^+	7.65420(15)	0.3795	$(8.5 \pm 1.0) \times 10^{-6}$	0.538	$\leqslant 2.2 \times 10^{-3}$	3.98
0_3^+	≈10.3	≈3	≈3	4.42	0.85	3.58
2_2^+	9.6(1)	2.33	0.6(1)	4.55	0.66	3.30
0_4^+				13.49	1.2	2.92
4_2^+				15.69	1.36	2.76
3_1^+				9.03	2	2.73
3_1^-	9.641(5)	2.366	0.034(5)	0.935	0.001	2.76
1_1^-	10.844(16)	3.569	0.315(25)	3.22	0.18	3.05
2_1^-	11.828(16)	4.553	0.260(25)	4.22	0.13	3.08
(4_1^-)	13.352(17)	6.077	0.375(40)	4.20	0.01	2.72
5_1^-				8.59	0.2	2.51
3_2^-				7.34	0.2	2.45
4_2^-				8.92	1.52	2.31

Such an expression for some general observables as the mean square radius or the mean kinetic energy turns out to be stable and independent of the complex-scaling angle θ. Furthermore, for narrow resonances, the complex mean-value integrals are generally dominated by the real parts. Therefore, when presenting results, we omit the small imaginary parts. Let us also notice that in the following the root-mean-square radius is computed by taking into account correction due to the finite size of the α particle $\sqrt{r^2} = \sqrt{r_C^2 + 1.71^2}$, where r_C^2 is the rms radius obtained with Eq. (9).

In the present work, the importance of each partial-wave Faddeev component is estimated by means of the A_{ℓ_x,ℓ_y} terms defined as follows:

$$A_{\ell_x,\ell_y} = \frac{3}{N} \iint \widetilde{\psi}_{ij,k}^{\ell_x,\ell_y}(\vec{x_{ij}}, \vec{y_{ij}}) \widetilde{\Psi}(\vec{x_{ij}}, \vec{y_{ij}}) d^3x_{ij} d^3y_{ij}, \quad (12)$$

where $\widetilde{\psi}_{ij,k}^{\ell_x,\ell_y}(\vec{x_{ij}}, \vec{y_{ij}})$ is given by

$$\widetilde{\psi}_{ij,k}^{\ell_x,\ell_y}(\vec{x_{ij}}, \vec{y_{ij}}) = \frac{\psi_{\ell_x\ell_y}^{LM}(x_{ij}, y_{ij})}{x_{ij} y_{ij}} \left[Y_{\ell_x}(\widehat{x_{ij}}) \otimes Y_{\ell_y}(\widehat{y_{ij}}) \right]_{LM}. \quad (13)$$

In general, the A_{ℓ_x,ℓ_y} terms are complex numbers, dominated by the real parts for narrow resonances. Mostly real parts A_{ℓ_x,ℓ_y} are positive and sum to unity, which is implied by the normalization factor $\frac{N}{3}$. Nevertheless, in some cases small negative A_{ℓ_x,ℓ_y} contributions are also possible.

III. RESULTS WITH THE PAPP AND MOSKOWSKI POTENTIAL

A. The 0_1^+, 2_1^+, and 4_1^+ ground-state rotational band

As aforementioned, Papp and Moszkowski [30] succeeded in parametrizing a nonlocal fish-bone-type potential that reproduces the 0_1^+ ground-state energy with respect to the 3α threshold without any three-body force. Along with the binding energy our calculations provide a 0_1^+ rms radius of 2.40 fm, which is close to the experimental value of $R \approx 2.47$ fm. This value is also in agreement with microscopic approaches where the 0_1^+ can be described either as 3α clusters located at the apexes of an equilateral triangle [42] or as a compact shell-model-like structure [9,11]. The analysis of the corresponding A_{ℓ_x,ℓ_y} terms (not shown here) reveals a mixed structure in the S, D, and G waves.

Regardless of the nice description of the 0_1^+ state, the 2_1^+ and 4_1^+ states are strongly overbound in our calculations (see Table I and Figs. 1 and 2). The 4_1^+ state is obtained as a bound state, while it is situated above the 3α threshold experimentally. However, let us notice that the 0_1^+, 2_1^+, and 4_1^+ sequence keeps a rotational band structure but with a too-small rotational constant (see Fig. 1). A similar drawback is also present for microscopic-cluster models and is interpreted as a lack of spin-orbit interaction [42].

The poor description of the ground-state band is not really surprising within a nonmicroscopic framework. This can be easily understood as a signature of the nonbosonic nature of these compact states, which apparently require a proper microscopic treatment.

B. 3α positive-parity resonances

The nonlocal Papp and Moszkowski potential reproduces fairly well the 0_2^+ Hoyle state (see Table I, and Figs. 1 and 2). For this state, our calculation provides a rms radius value of 3.98 fm compatible with the analysis of electron inelastic scattering data [44] as well as other theoretical models [11,14,16]. It also confirms the interpretation of the 0_2^+ state as a 3α dilute state. Let us remark that the numerical accuracy of our calculation is not enough to determine the width of very

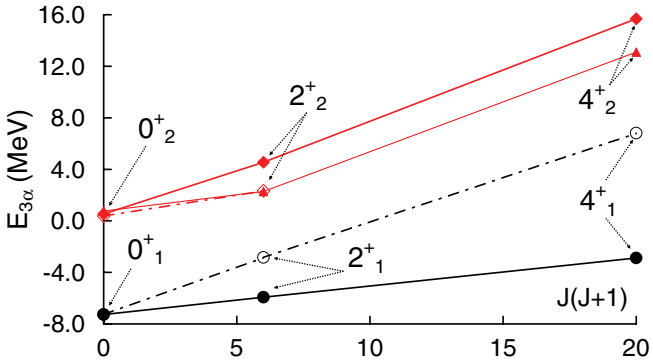

FIG. 1. (Color online) Ground-state rotational band (black circles) and 0_2^+ Hoyle-state rotational band (red diamonds) are obtained with the nonlocal Papp and Moszkowski potential. The 0_2^+ band calculated by Kurukawa and Katō [16] (red triangles) is also given. Solid symbols and solid lines correspond to calculated values. Open symbols and dotted lines correspond to experimental data taken from Ref. [36] for the 2_2^+ data and from Ref. [43] for the other data.

narrow resonances such as the Hoyle state. In such a case, we just provide an upper value.

A very interesting point related to our study with the nonlocal Papp and Moszkowski potential is the existence of a set of states $\{0_2^+, 2_2^+, 0_3^+, 0_4^+, 4_2^+\}$ which share intriguing common features.[1] In particular, the analysis of the A_{ℓ_x,ℓ_y} terms gathered in Table II shows that respective wave functions are dominated by a single partial wave with $\ell_x = \ell_y$. In general, ℓ_x and ℓ_y are not good quantum numbers and the A_{ℓ_x,ℓ_y} values are necessarily potential dependant. However, their quasiuniqueness in the case of the nonlocal Papp and Moszkowski potential points out a common denominator between the states that is interesting to discuss. Indeed, condensates such as the Hoyle state are usually described as a dilute bosonic state with zero angular-momentum values between the α particles (see Refs. [14,38] and references therein). Our calculation confirms this property for the 0_2^+ state. Furthermore, the possibility of condensate states with nonzero angular momentum, as discussed in Ref. [14], appears also relevant. In such a context, and due to the interpretation of the Hoyle state as condensate, the previous set of states can be interpreted as a same family of 3α-condensate states differentiated by the relative angular-momentum values.

Let us now discuss each member of the condensate family in more detail. To facilitate the comparison with our results, results of the two nonmicroscopic works of Yamada and Schuck [14] and Kurukawa and Katō [16] are also gathered in Fig. 3. Let us remind that in both cases three-body forces are used at least to reproduce the ^{12}C ground state with respect to the 3α threshold. Furthermore, the three-body forces used in Ref. [16] are J dependent and are fitted to reproduce the ground-state band.

[1]Here, subscripts 2, 3, and 4 refer to the order of the states with respect to the calculated energy.

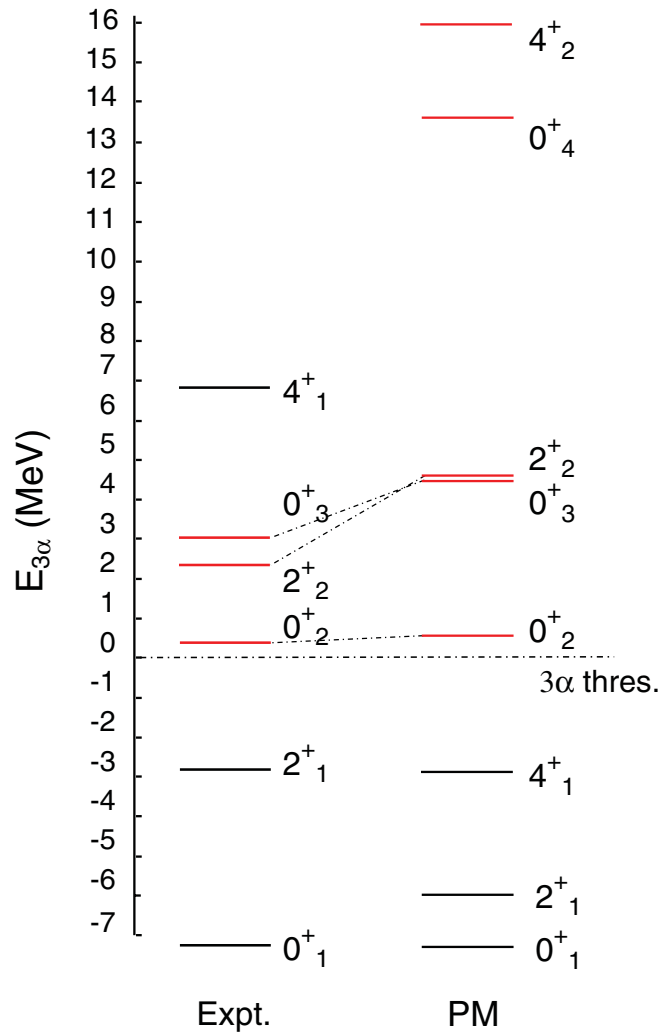

FIG. 2. (Color online) Ground-state band (black) and positive-parity condensate states (red) obtained with the nonlocal Papp and Moszkowski potential (PM). Corresponding experimental data (Expt.) are taken from Ref. [36] for the 2_2^+ and from Ref. [43] for the other data.

The 2_2^+ state at 4.55 MeV with a width of 0.66 MeV and a dominant $A_{2,2}$ term can be interpreted as the 2^+ member of the Hoyle-state band. Its energy is overestimated by ≈2 MeV as compared to the measure of Freer *et al.* [36]. We also assign the 4_2^+ state with a dominant $A_{4,4}$ term to a possible 4^+ member of the Hoyle-state band. The corresponding rotational band is plotted in Fig. 1. We can notice the fairly nice alignment, regardless of the fact that the 2_2^+ and 4_2^+ states are quite broad already. The rotational constant, however, is overestimated compared to the corresponding one obtained with the 2^+ experimental value of Freer *et al.* [36]. It is worth mentioning that, in the corresponding resonances calculated by Kurukawa and Katō [16], such rotational band structure does not prevail and is spoiled by the J dependance of the three-body forces (see Fig. 1). Our calculation indicates the existence of a 0_3^+ resonance at 4.42 MeV above the 3α threshold, close to the 2_2^+ state. Its direct assignment to the broad 0^+ resonance experimentally suggested at ≈3

TABLE II. $[\ell_x, \ell_y]$ value of the dominant A_{ℓ_x,ℓ_y} term with respective magnitude in parentheses for positive-parity states referred as condensates in the text. For negative-parity states, the two dominant values are given with respective magnitude in parentheses.

J^π	$[\ell_x, \ell_y]$
0_2^+	[0, 0] (0.96)
0_3^+	[2, 2] (1.0)
0_4^+	[4, 4] (0.82)
2_2^+	[2, 2] (0.94)
4_2^+	[4, 4] (0.80)
1_1^-	[2, 1] (0.68), [2, 3] (0.15)
2_1^-	[2, 1] (0.54), [2, 3] (0.35)
3_1^-	[2, 1] (0.56), [0, 3] (0.26)
4_1^-	[2, 3] (0.65), [4, 1] (0.22)
5_1^-	[4, 3] (0.51), [4, 1] (0.15)

MeV above the 3α threshold with an estimated width of $\approx$3 MeV [37,43] cannot be justified. On the one hand, it makes no sense to compare effective parameters of such broad resonances with S-matrix pole positions found in theoretical calculations, because such resonances may not be interpreted as Breit-Wigner ones. On the other hand, the complex-scaling method is not adapted to describe very broad resonances (see also discussions in Ref. [15]). Nevertheless, we confirm the existence of a 0^+ resonance with a bosonic α structure in the energy range of the 2_2^+ state in agreement with Kurukawa and Katō [16], who predict the same states but at lower energy. New experimental investigations would be useful in this energy range to clarify the properties of these broad states.

It is also interesting to notice that our calculations reproduce a 0_4^+ resonance at $E_{3\alpha} = 13.49$ MeV with a dominant $A_{4,4}$ term. Furthermore, if we represent the energies of the aforementioned condensate 0^+ states as a function of $\ell(\ell+1)$, with $\ell = \ell_x = \ell_y$, we get a nice alignment (see Fig. 4) pointing

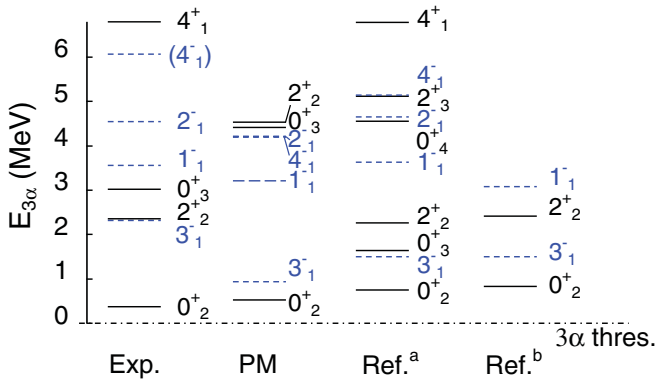

FIG. 3. (Color online) 3α positive-parity resonances (black full lines) and negative-parity resonances (blue dashed lines) obtained with the nonlocal Papp and Moszkowski potential (PM) compared with the results of Kurukawa and Katō [16] and the results of Yamada and Schuck [14]. Corresponding experimental data (Expt.) are taken from Ref. [36] for the 2_2^+ state and from Ref. [43] for the other data.

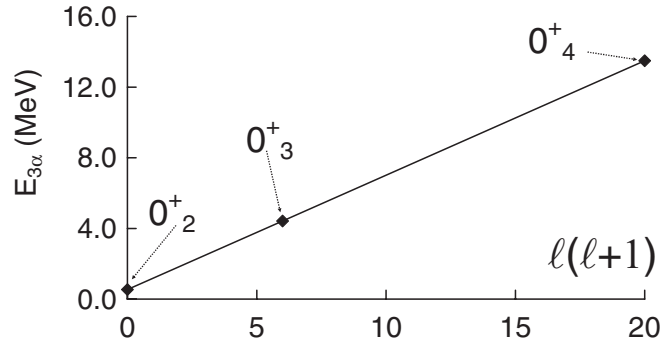

FIG. 4. 0^+ condensate state energies obtained with the nonlocal Papp and Moskowski potential as a function of $\ell(\ell+1)$.

out a rotational band structure. It would be interesting to test this result experimentally.

The values of the radii gathered in Table I are also consistent with our condensate-state interpretation. Indeed, resonance radii are greater than those of the bound states. We can also see the obvious effect of the centrifugal barrier with $\ell = 2$ for the 0_3^+ and 2_2^+ states and $\ell = 4$ for the 0_4^+ and 4_2^+ states. Indeed, states dominated by the same efficient centrifugal term (ℓ) have very similar extensions. Large centrifugal terms permit to reduce the mean radii regardless of the fact that resonances are pushed further into the continuum as ℓ increases.

Let us finally remark that our calculations indicate the existence of a broad positive-parity 3^+ resonance at $E_x = 9.03$ MeV, which cannot be interpreted as a condensate.

C. 3α negative-parity resonances

Negative-parity resonances are also well reproduced with the nonlocal Papp and Moszkowski potential (see Tables I and II, and Figs. 5 and 6). This is especially the case for the 3_1^-, 1_1^-, and 2_1^- states, which are known to present marked α structure [14,16,38]. However, the analysis of the A_{ℓ_x,ℓ_y} coefficients gathered in Table II shows a rather mixed structure, which prevents straightforward interpretation in terms of condensate. Similarly, the radius of the 3_1^-, 2_1^-, and 1_1^- states being intermediate between the radius of bound and condensate states, in agreement with Ref. [14], leads to similar conclusions.

In addition, the 3_1^- state is also believed to be the head of a $K = 3^-$ rotational band in microscopic-cluster studies [42]. Up to now, there is no experimental evidence for 4^- and 5^- states which could belong to this band. Our calculation suggests a $K = 3^-$ band along with the calculated 4_1^- and 5_1^- members. The corresponding band is plotted in Fig. 6. In such a context, it is consistent to assign the 4_1^- resonance obtained in our calculations to the level at $E_x = 13.352$ MeV tentatively assigned to 2^- in Ref. [43], as proposed by Kurukawa and Katō (see discussion in Ref. [16]).

Let us also remark that our calculation points out other negative-parity resonances (3_2^-, 4_2^-) that have not been experimentally observed yet.

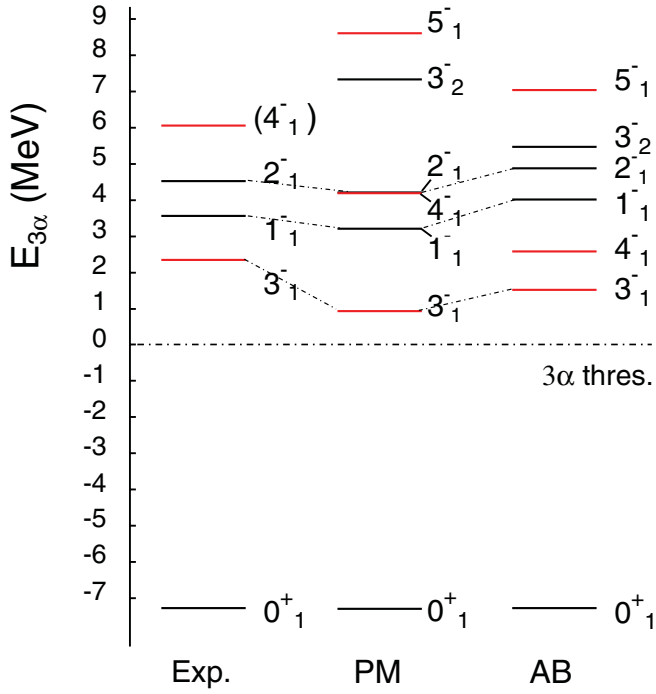

FIG. 5. (Color online) 3α negative-parity resonances obtained with the nonlocal Papp and Moszkowski potential (PM) and the Ali and Bodmer potential (AB). States corresponding to the $K = 3^-_1$ rotational band are colored in red. Corresponding experimental data (Expt.) are taken from Ref. [36], where the (4^-_1) at $E_x = 13.352$ MeV is tentatively assigned to a 2^- state (see text).

IV. COMPLEMENTARY INVESTIGATIONS WITH THE ALI AND BODMER POTENTIAL

As discussed in the introduction, the local Ali and Bodmer α-α potential [19] fails to provide enough binding for ^{12}C positive-parity states. For such a model, positive-parity resonances are naturally pushed far into the continuum. The standard way to improve the description is to introduce a three-body force to simulate the effect of additional

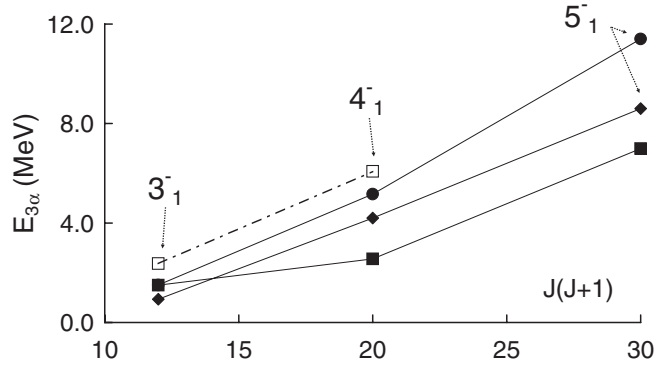

FIG. 6. $K = 3^-_1$ rotational band obtained with the Ali and Bodmer potential (solid squares) and with the nonlocal Papp and Moszkowski potential (solid diamonds). Corresponding results of Kurukawa and Katō [36] are also given (solid circles). Experimental data (open squares) are taken from Ref. [36], where the (4^-) at $E_x = 13.352$ MeV is tentatively assigned to a 2^- state (see text).

TABLE III. ^{12}C energies (in MeV), total widths (in MeV) and root-mean-square radius (in Fermi) calculated with the Ali and Bodmer potential (AB). Experimental data are taken from Ref. [43] where the (4^-) at $E_x = 13.352$ MeV is tentatively assigned to a 2^- state (see text).

J^π	$E_x^{\rm expt}$	$E_{3\alpha}^{\rm expt}$	$\Gamma^{\rm expt}$	$E_{3\alpha}^{\rm AB}$	$\Gamma^{\rm AB}$	$\sqrt{r^2}^{\rm AB}$
3^-_1	9.641(5)	2.366	0.034(5)	1.50	0.7×10^{-3}	2.83
1^-_1	10.844(16)	3.569	0.315(25)	3.97	0.52	3.37
2^-_1	11.828(16)	4.553	0.260(25)	4.85	.58	3.29
(4^-_1)	13.352(17)	6.077	0.375(40)	2.56	2.6×10^{-3}	2.49
5^-_1				6.99	0.58	2.90
3^-_2				5.44	0.55	2.30
4^-_2				7.12	1.92	3.01

polarization due to the presence of the third α particle. Several works are devoted to this subject (see, for example, Refs. [2,17,18,20] and references therein). However, they all failed to parametrize simple three-body forces capable of reproducing simultaneously the 0^+_1 ground state and 2^+_1 excited states of the ^{12}C nucleus.

Following this track, we have also tried to complement the Ali and Bodmer potential with three-body force depending on the hyper-radius of the three-body system ($\rho_3^2 = 4\sum_i r_i^2$). More precisely, three different forms have been tested: a Gaussian expression as used in Refs. [18,45], a Woods-Saxon expression, and a Yukawa form. However, all these tests provide very similar results. Indeed, owing to the lack of a centrifugal barrier, the 0^+ states are more extended than the other positive-parity states, such as the 2^+ or 4^+ states, and thus less sensitive to the three-body interaction. Therefore, the lowest 2^+ and 4^+ states are rapidly overbound. In addition, some resonances, such as the 3^- and 4^- states, for instance, turn out to be very sensitive to the three-body force and become bound. For example, with the Gaussian parametrization defined in Ref. [18] with $v_3 = -22$ MeV and $\rho_3 = 6$ fm, we get the ^{12}C 2^+_1 state bound by 6.3 MeV as well as the 3^-_1 state bound by 5.3 MeV.

Let us nevertheless remark that, in spite of the failure to describe positive-parity ^{12}C states, the Ali and Bodmer potential alone provides a very reasonable description of negative-parity resonances (see Table III and Figs. 5 and 6). Our calculations show rather similar results compared to those obtained with the Papp and Moszkowski potential. Nevertheless, the Ali and Bodmer energy values are slightly more condensed and the rotational alignment of 3^-_1, 4^-_1, and 5^-_1 states is not preserved, which is probably because of the fact that the Ali and Bodmer potential is strongly partial wave dependent (see Fig. 6).

V. CONCLUSIONS

The interplay between the fermionic and bosonic descriptions of the same composite system such as a nucleus is a very interesting challenge. In particular, it can help to point out states with important bosonic clustering such as in the so-called condensates, a typical example being the ^{12}C 0^+_2 Hoyle state.

In this paper, we mainly investigated the ^{12}C spectrum within a 3α nonmicroscopic model based on the rigorous solution of the Faddeev equations for the nonlocal Papp and Moszkowski α-α potential. Our calculations point out a set of states $\{0_2^+, 2_2^+, 0_3^+, 0_4^+, 4_2^+\}$ which share common features with the 0_2^+ Hoyle state. Negative-parity states around the 3α threshold are also well reproduced by both the nonlocal Papp and Moszkowski potential and the Ali and Bodmer potential.

The nonlocal Papp and Moszkowski potential appears to be a very efficient tool to investigate the physics of the 3α bound and resonant states. We emphasize that all the results published here were obtained without resorting to three-body potentials and/or adding explicit angular-momentum dependence. This result encourages us to pursue nonmicroscopic investigations within the same framework. In such a context, we aim to investigate the possible existence of condensate states in the 4α system.

ACKNOWLEDGMENTS

We would like to thank Z. Papp, P. Descouvemont, and P. Schuck for stimulating discussions. For this work we were granted access to the HPC resources of IDRIS under the Grant No. 2009-i2009056006 made by GENCI (Grand Equipement National de Calcul Intensif). We thank the staff members of the IDRIS for their constant help.

[1] P. Ring and P. Schuck, *The Nuclear Many-Body Problem* (Springer, New York, 1980).
[2] D. M. Brink, J. Phys. Conf. Ser. **111**, 012001 (2008).
[3] P. Descouvemont and M. Dufour, *Clusters in Nuclei, Vol. 2*, Lecture Notes in Physics (Springer, in press).
[4] J. A. Wheeler, Phys. Rev. **52**, 1083 (1937).
[5] H. Margenau, Phys. Rev. **59**, 37 (1941).
[6] D. Brink, Proc. Int. Sch. Phys. "Enrico Fermi" **36**, 247 (1966).
[7] A. Tohsaki, H. Horiuchi, P. Schuck, and G. Röpke, Phys. Rev. Lett. **87**, 192501 (2001).
[8] F. Hoyle, Astrophys. J. Suppl. Ser. **1**, 121 (1954).
[9] M. Kamimura, Nucl. Phys. A **351**, 456 (1981).
[10] P. Descouvemont and D. Baye, Nucl. Phys. A **463**, 629 (1987).
[11] H. Horiuchi, *Clusters in Nuclei, Vol. 1*, Lecture Notes in Physics, Vol. 818 (Springer, Berlin, 2011).
[12] M. Chernykh, H. Feldmeier, T. Neff, P. von Neumann-Cosel, and A. Richter, Phys. Rev. Lett. **98**, 032501 (2007).
[13] S. Saito, Prog. Theor. Phys. Suppl. **62**, 11 (1977).
[14] T. Yamada and P. Schuck, Eur. Phys. J. A **26**, 185 (2005).
[15] C. Kurokawa and K. Katō, Phys. Rev. C **71**, 021301 (2005).
[16] C. Kurokawa and K. Katō, Nucl. Phys. A **792**, 87 (2007).
[17] R. Alvarez-Rodriguez, E. Garrido, A. S. Jensen, D. V. Fedorov, and H. O. U. Fynbo, Eur. J. Phys. A **31**, 303 (2007).
[18] P. Descouvemont, J. Phys. G **37**, 064010 (2010).
[19] S. Ali and A. R. Bodmer, Nucl. Phys. **80**, 99 (1966).
[20] Y. Suzuki, H. Matsumura, M. Orabi, Y. Fujiwara, P. Descouvemont, M. Theeten, and D. Baye, Phys. Lett. B **659**, 160 (2008).
[21] B. Buck, H. Friedrich, and C. Wheatley, Nucl. Phys. A **275**, 246 (1977).
[22] H. Matsumura, M. Orabi, Y. Suzuki, and Y. Fujiwara, Nucl. Phys. A **776**, 1 (2006).
[23] E. M. Tursunov, D. Baye, and P. Descouvemont, Nucl. Phys. A **723**, 365 (2003).
[24] M. Theeten, H. Matsumura, M. Orabi, D. Baye, P. Descouvemont, Y. Fujiwara, and Y. Suzuki, Phys. Rev. C **76**, 054003 (2007).
[25] Y. Fujiwara, M. Kohno, and Y. Suzuki, Few-Body Syst. **34**, 237 (2004).
[26] Y. Funaki, T. Yamada, H. Horiuchi, G. Röpke, P. Schuck, and A. Tohsaki, Phys. Rev. Lett. **101**, 082502 (2008).
[27] D. A. Zaikin, Nucl. Phys. A **170**, 584 (1971)
[28] E. W. Schmid, Z. Phys. A **297**, 105 (1980).
[29] E. W. Schmid, S. Saito, and H. Fiedeldey, Z. Phys. A **306**, 37 (1982)
[30] Z. Papp and S. Moszkowski, Mod. Phys. Lett. B **22**, 2201 (2008).
[31] L. D. Faddeev, Zh. Eksp. Teor. Fiz. **39**, 1459 (1960) [Sov. Phys.—JETP **12**, 1014 (1961)].
[32] J. Nuttal and H. L. Cohen, Phys. Rev. **188**, 1542 (1969).
[33] N. Moiseyev, Phys. Rep. **302**, 212 (1998)
[34] P. Navrátil, J. P. Vary, and B. R. Barrett, Phys. Rev. C **62**, 054311 (2000).
[35] E. Epelbaum, H. Krebs, D. Lee, and Ulf.-G. Meißner, Phys. Rev. Lett. **106**, 192501 (2011).
[36] M. Freer *et al.*, Phys. Rev. C **80**, 041303 (2009).
[37] M. Itoh *et al.*, Nucl. Phys. A **738**, 268 (2004).
[38] T. Yamada, P. Schuck, Y. Funaki, H. Horiuchi, G. Röpke, and A. Tohsaki, in *Clusters in Nuclei, Vol. 2*, Lecture Notes in Physics (Springer, in press).
[39] R. Lazauskas, Ph.D. thesis, Université Joseph Fourier, France, 2003 (unpublished), [http://tel.ccsd.cnrs.fr/documents/archives0/00/00/41/78/]
[40] R. Lazauskas and J. Carbonell, Phys. Rev. C **71**, 044004 (2005).
[41] C. de Boor, *A Practical Guide to Splines* (Springer-Verlag, Berlin, 1978).
[42] M. Dufour and P. Descouvemont, Nucl. Phys. A **605**, 160 (1996).
[43] F. Ajzenberg-Selove, Nucl. Phys. A **506**, 1 (1990).
[44] Y. Funaki, A. Tohsaki, H. Horiuchi, P. Schuck, and G. Röpke, Eur. J. Phys. A **28**, 259 (2006).
[45] D. V. Fedorov and A. S. Jensen, Phys. Lett. B **389**, 631 (1996).